

Available online at [www.sciencedirect.com](http://www.sciencedirect.com)

ScienceDirect

[www.elsevier.com/locate/jes](http://www.elsevier.com/locate/jes)

**JES**  
 JOURNAL OF  
 ENVIRONMENTAL  
 SCIENCES  
[www.jesc.ac.cn](http://www.jesc.ac.cn)

# Effects of temperature and SO<sub>3</sub> on re-emission of mercury from activated carbon under flue gas conditions

Michael Royko<sup>1</sup>, Benjamin Galloway<sup>1</sup>, Noah D. Meeks<sup>2</sup>, Bihter Padak<sup>1,\*</sup>

1. Department of Chemical Engineering, University of South Carolina, 541 Main St., Columbia, SC 29201, USA

2. Southern Company Services, Inc. 600 18th Street North, Birmingham, AL 35203, USA

## ARTICLE INFO

### Article history:

Received 21 June 2018

Revised 15 October 2018

Accepted 23 October 2018

Available online 30 October 2018

### Keywords:

Mercury re-emission

Sulfur trioxide

Activated carbon

## ABSTRACT

Mercury (Hg) is a toxic and bio-accumulating heavy metal that is predominantly released via the combustion of coal. Due to its toxicity, the Environmental Protection Agency (EPA) has introduced Mercury and Air Toxics Standards (MATS) Rule regarding allowable Hg emissions. In order to reduce emissions, power plants have widely adopted activated carbon (AC) injection. AC injection has proven to be an effective method to reduce Hg emissions, but the re-emission of previously adsorbed Hg during unit operation, likely due to changing temperature or flue gas composition, could be problematic. This study specifically examined the effects of temperature and sulfur trioxide (SO<sub>3</sub>) concentration, by ramping temperature and SO<sub>3</sub> concentration independently and simultaneously, on AC samples that are already exposed to flue gas and saturated in presence of Hg, sulfur dioxide (SO<sub>2</sub>) and nitric oxide (NO). Of these two suspected factors to cause re-emission, temperature had the greater impact and resulted in re-emission of both elemental and oxidized Hg with a greater fraction of oxidized Hg, which can be attributed to elemental Hg being more strongly bonded to the AC surface. Surprisingly, exposing the samples to increasing concentrations of SO<sub>3</sub> had nearly no effect under the conditions examined in this study, possibly as a result of the samples being already saturated with sulfur prior to the SO<sub>3</sub> ramp tests to simulate transient conditions in the plant.

© 2018 The Research Center for Eco-Environmental Sciences, Chinese Academy of Sciences.

Published by Elsevier B.V.

## Introduction

While electrical generators based on solar PV, wind, and natural gas are prominent, coal still accounts for upwards of 30% of the energy production in the United States in 2017 (EIA, 2018). Coal combustion results in the formation of various pollutants, which are controlled through electrostatic precipitators, baghouses, selective catalytic or non-catalytic reduction (SCR or SCNR) units, and wet or dry flue gas desulfurization

(FGD) scrubbers. However, mercury is not well-controlled using conventional air pollution control equipment. In fact, over 22.8 tons of mercury (Hg) were released from coal-fired power plants in the United States in 2014 alone (Bolate, 2017). This is especially troubling as Hg is a severe neurotoxin and is persistent in the environment (Kampa and Castanas, 2008; Rice et al., 2014). In order to address these concerns, the Environmental Protection Agency (EPA) introduced the Mercury and Air Toxic Standards (U.S.EPA, 2011) which calls for the

\* Corresponding author. E-mail: [padak@cec.sc.edu](mailto:padak@cec.sc.edu). (Bihter Padak).

capture and removal of 90% of the Hg from coal-fired power plants. Process conditions greatly impact Hg speciation in the flue gas. In commercial power plants there are three different forms of Hg, each with their own degree of difficulty of removal from the flue gas. Oxidized ( $\text{Hg}^{2+}$ ) and particulate bound ( $\text{Hg}^p$ ) are the easiest to capture as  $\text{Hg}^{2+}$  is water soluble and can be removed in wet flue gas desulfurization units while  $\text{Hg}^p$  is removed in particulate removal devices when the solid particles are removed from the flue gas (Yan et al., 2003). However, there are considerable difficulties with the removal of elemental Hg ( $\text{Hg}^0$ ). To this end a number of various techniques ranging from sorbents (Granite et al., 1998; Ghorishi and Sedman, 1998; Granite et al., 2000; Ralston, 2008) to oxidation catalysts (Eswaran and Stenger, 2005; Kamata et al., 2009; Presto and Granite, 2008) have been investigated for their ability to reduce Hg emissions.

Of particular interest are activated carbon (AC) sorbents as they are used commercially and have been proven to be effective for Hg capture. While these sorbents can be produced from various forms of biomass (De et al., 2013; Min et al., 2017; Rungrim et al., 2016; Tan et al., 2012; Zhu et al., 2016) or coal fly ash (Granite et al., 2007; Qiao et al., 2009), most often the industry uses AC produced from lignite coal. Often times the AC is treated with an additional component such as sulfur (Korpiel and Vidic, 1997; Mullett et al., 2012; Sano et al., 2017) or halogens (Rungrim et al., 2016; Rupp and Wilcox, 2014; Sano et al., 2017; Sasmaz et al., 2012; Zhu et al., 2016) to improve Hg capture performance. However, the performance of these sorbents are highly dependent on flue gas conditions such as temperature and gas composition and how these conditions interact with the carbon sorbent itself. Therefore, a number of studies have investigated the impact of temperature (Ho et al., 1998) and flue gas composition (Miller et al., 2000; Ochiai et al., 2009; Presto and Granite, 2007; Presto et al., 2007; Sjostrom et al., 2009; Yan et al., 2003) on the efficacy of the sorbent. Of these additional flue gas components, sulfur oxides are of particular interest. Although there is a complex relationship between the addition of sulfur oxides and sorbent performance, in general, the addition of these compounds has a deleterious impact on sorbent activity due to the competition of sulfur oxides and  $\text{Hg}^{2+}$  for the same Lewis base binding site on the AC (Presto and Granite, 2007). Furthermore, it has been found that sulfur trioxide ( $\text{SO}_3$ ) has a stronger effect than sulfur dioxide ( $\text{SO}_2$ ) (Presto and Granite, 2007; Presto et al., 2007; Sjostrom et al., 2009). In addition, Hg capture has been shown to be inversely related to temperature (Ho et al., 1998; Luo et al., 2006) and temperature programmed desorption has been widely utilized to analyze the chemical identity of Hg that is released from AC (Rumayor et al., 2015; Senior et al., 2010; Sun et al., 2017; Zhou et al., 2017). Recent work by the Electric Power Research Institute (EPRI) demonstrated that re-emission of mercury occurred in a TOXECON baghouse (pulse-jet fabric filter with mercury sorbent injection) likely due to temperature increase, sulfuric acid mist, and increase in AC loading (EPRI, 2015). It is important to understand the underlying phenomena causing this issue so that engineering measures can be taken to address it. Therefore, the objective of this study is to determine the cause(s) of Hg re-emission from an AC sorbent under realistic power plant conditions, namely temperature and  $\text{SO}_3$  concentration ramps, in a controlled environment.

## 1. Materials and methods

A schematic of the experimental setup used for this study is displayed in Fig. 1. This experimental setup utilizes a PS Analytical CavKit Hg Vapor Generator to provide a Hg containing air stream, which is mixed with methane and combusted in a quartz burner heated to  $1100^\circ\text{C}$ . Hg concentration was measured using a PS Analytical Sir Galahad Hg analyzer equipped with a PS Analytical Cracker Probe Hg speciation system. The system was calibrated using a two-point calibration before each experiment. Complete combustion of methane in excess air in the burner provides a simulated flue gas stream with an estimated composition of 74%  $\text{N}_2$ , 6%  $\text{O}_2$ , 6.5%  $\text{CO}_2$  and 13.5%  $\text{H}_2\text{O}$ , which serves as the base flue gas for all of the experiments. Downstream of the furnace, additional flue gas components can be added to the combustion products before entering the reactor. All additional flue gas components were provided from gas tanks that are commercially available except for  $\text{SO}_3$ , which was produced in house via the oxidation of  $\text{SO}_2$  over an oxidation catalyst. The catalyst was heated and exposed to a stream of  $\text{SO}_2/\text{air}$  for at least 30–60 min prior to feeding the freshly made  $\text{SO}_3$  into the simulated flue gas in order to ensure that the catalyst has equilibrated. The concentration of  $\text{SO}_3$  was determined via the salt method (Vainio et al., 2013) before running the experiments and was checked periodically to ensure accuracy. The catalyst was replaced with a fresh one and the new activity was checked every four runs, which occurred every 2 days.

The burner is followed by a quartz packed-bed reactor that contains 2 mg AC sample mixed with 1 g sand (100–250  $\mu\text{m}$ ). The powdered AC that was used in this study is PowerPAC Premium from ADA Carbon Solutions, an industry-leading supplier of AC to the coal-fired electric generation industry. PowerPAC Premium is a standard, early generation brominated AC that is typically used in a baghouse application.

In order to properly simulate Hg re-emission as would be experienced in a power plant setting, the AC samples were first saturated with Hg before subjecting the samples to any ramps representing changes that might occur during power plant operation. In order to saturate the samples with Hg, the

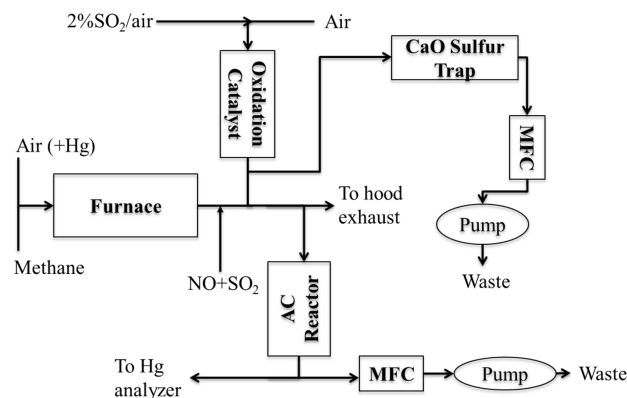


Fig. 1 – Schematic of the experimental setup.

samples were loaded into the reactor and heated to 150°C. The samples were saturated with Hg at this temperature under the previously mentioned combustion products with the addition of 200 ppm SO<sub>2</sub>, 50 ppm NO and 100 µg/m<sup>3</sup> of Hg, which takes approximately 1.5–2 hr to complete. In order to simulate conditions that could cause Hg re-emission from saturated AC sorbents in power plants, the sorbents were subjected to conditions in which temperature, SO<sub>3</sub> concentration, or both were increased (ramped) over time. For the temperature ramp (T-ramp) experiments, after exposure to Hg at 150 °C the sample was first cooled to 105°C before heating to 205°C at a rate of 3.33°C per minute while the SO<sub>3</sub> concentration was kept constant at 5 ppm. Due to concerns over H<sub>2</sub>O or H<sub>2</sub>SO<sub>4</sub> condensation, the ramp could not begin from ambient temperature. Furthermore, to prevent condensation in the gas lines, all lines were heated via heat tapes to 150°C–200°C. For the SO<sub>3</sub> concentration ramp experiments (SO<sub>3</sub>-ramp), the temperature was kept constant at 150°C while the SO<sub>3</sub> concentration was changed step-wise every 4.8 min (the time required for the Hg analyzer to take a sample) from 2 to 20 ppm. This was done by adjusting the split fraction of the flow from the oxidation catalyst to the simulated flue gas stream. In this way, the catalyst was kept under constant gas flow and composition for the duration of the exposure while allowing variable SO<sub>3</sub> concentrations to be fed to the reactor housing the AC sample. In order to protect downstream equipment, a CaO trap was inserted to capture excess SO<sub>3</sub> before it goes to exhaust. For the runs where both temperature and SO<sub>3</sub> concentration were ramped (T + SO<sub>3</sub>-ramp), the sample was first cooled to 105°C before introducing the SO<sub>3</sub>. For these cases, the procedure was slightly altered from the temperature-only ramp. The T + SO<sub>3</sub>-ramp's SO<sub>3</sub> concentration profile was the same as the only SO<sub>3</sub>-ramp; however, the temperature ramp was delayed to account for the slightly different lengths of the two procedures.

## 2. Results and discussion

### 2.1. Saturation of activated carbon with mercury

Prior to investigating the AC samples under the various ramp conditions, several tests were conducted to optimize the test conditions. The results from the first set conducted under combustion products only (N<sub>2</sub>, O<sub>2</sub>, H<sub>2</sub>O, and CO<sub>2</sub>) are presented in Fig. 2. The graph shows the breakthrough curves for Hg through the AC bed for a variety of Hg concentrations. Within the timescale shown, only the two highest concentrations, 1236 and 305 µg/m<sup>3</sup>, achieve breakthrough within a single exposure experiment (~4 hr), resulting in final Hg loadings of 16.7 and 13.4 mg Hg/g AC, respectively. While the lowest value, 42 µg/m<sup>3</sup>, is a more realistic Hg concentration found in power plants, the sample does not reach breakthrough in this timescale. The final amount of Hg captured under these conditions is 6.2 mg Hg/g AC indicating that it would take significantly longer to reach saturation. After the baseline performance was established, additional flue gas components were added to more realistically simulate flue gas as some of the flue gas constituents influence Hg capture.

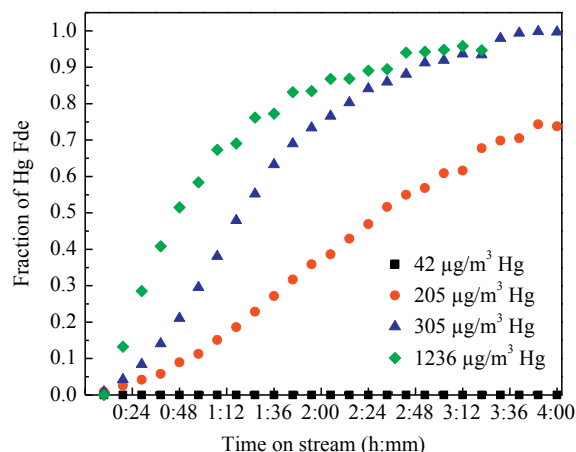


**Fig. 2 – Breakthrough curves for activated carbon samples exposed to Hg in combustion products (CO<sub>2</sub> + H<sub>2</sub>O + N<sub>2</sub> + O<sub>2</sub>) with various Hg concentrations at 150 °C.**

Particularly, sulfur limits the adsorption of Hg on AC (Carey et al., 1998; Ochiai et al., 2009; Rupp and Wilcox, 2014) due to the competition of SO<sub>x</sub> and Hg<sup>2+</sup> for the same binding site on the carbon surface (Li et al., 2017; Presto and Granite, 2007). Therefore, 200 ppm of SO<sub>2</sub> and 50 ppm of NO were added to the combustion products in order to have a more realistic flue gas composition. The results from these experiments are presented in Fig. 3. The breakthrough graphs differ from the ones conducted under only combustion products in one important aspect. They show the decrease in the timescale required for saturation, where the AC fully saturates in around 2 h under a Hg concentration as low as 100 µg/m<sup>3</sup>, where the total amount captured decreased to less than 2 mg Hg/g AC. Despite being higher than what would be characteristic of flue gas, 100 µg/m<sup>3</sup> was chosen as a representative Hg

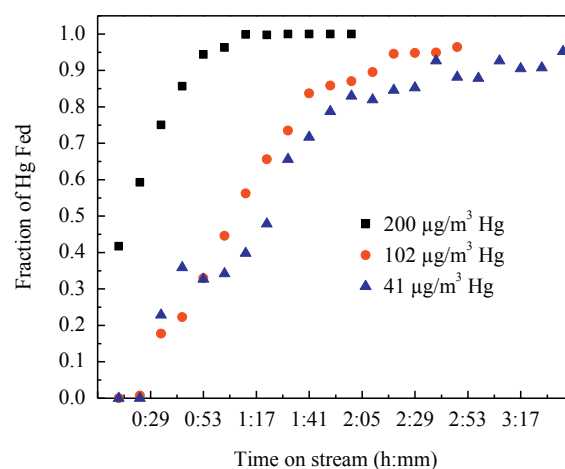


**Fig. 3 – Breakthrough curves for activated carbon samples exposed to Hg in simulated flue gas (CO<sub>2</sub> + H<sub>2</sub>O + N<sub>2</sub> + O<sub>2</sub> + 50 ppm NO + 200 ppm SO<sub>2</sub>) with various Hg concentrations at 150 °C.**

concentration for this study to facilitate reasonable saturation times.

## 2.2. Effect of temperature and $\text{SO}_3$ concentration on mercury re-emission

As mentioned previously, three different ramps were employed ( $\text{SO}_3$ , T, and T +  $\text{SO}_3$ ) for the investigation of the re-emission of Hg from AC after the samples are saturated at  $150^\circ\text{C}$ . The Hg concentration profiles obtained during saturation are not shown in the figures presented in this section for the ramp experiments, as the saturation portion is consistent from sample to sample and is similar to what is shown in Fig. 3.

### 2.2.1. Change in $\text{SO}_3$ concentration ( $\text{SO}_3$ -ramp)

Fig. 4 presents the data for two sets of runs (four samples) conducted applying a ramp in the  $\text{SO}_3$  concentration from 2 to 20 ppm at  $150^\circ\text{C}$  after the samples were saturated. The graph shows the results for both total Hg ( $\text{Hg}^{\text{T}}$ ) and elemental Hg ( $\text{Hg}^0$ ) measured using the Hg analyzer. The third set of data is oxidized mercury ( $\text{Hg}^{2+}$ ) and was calculated as the difference between  $\text{Hg}^{\text{T}}$  and  $\text{Hg}^0$ . Lastly, the dotted line labeled “Hg Fed” represents the concentration of Hg being fed to the reactor and is at  $100 \mu\text{g}/\text{m}^3$ . As the analyzer cannot measure both total and elemental Hg simultaneously, alternating runs were performed where either total or elemental Hg was measured. Additionally, to account for experimental error, the order of the total and elemental Hg measurements was switched from day to day, e.g., one day the experiment was first conducted by measuring elemental Hg followed by the experiment measuring total Hg and the other day the total Hg measurement was conducted first followed by elemental Hg. This is indicated on the graphs by the suffix “-1” or “-2”, where the

number indicates whether it was run first or second on its respective day.

There are two main conclusions to be extracted from Fig. 4. The first is the change in  $\text{Hg}^{\text{T}}$  relative to the feed concentration as it can represent either re-emission (above feed line) or increased capture (below feed line). From the two  $\text{Hg}^{\text{T}}$  lines, it is discernible that  $\text{SO}_3$  does not seem to appreciably affect Hg adsorption in this experiment; neither benefiting nor impairing the sorbent's capacity to a great extent. While some fluctuation is observed from point to point, the change can be considered negligible when accounting for experimental error. Secondly, just like the  $\text{Hg}^{\text{T}}$  profiles, the  $\text{Hg}^0$  ones show little change with respect to  $\text{SO}_3$  concentration, despite being at different values from run to run. The stable  $\text{Hg}^0$  and  $\text{Hg}^{\text{T}}$  levels indicate that the change in  $\text{SO}_3$  concentration not only does not affect the release of Hg from the sorbent but it also does not affect the oxidation activity of the material, evident from the minimally changing  $\text{Hg}^{2+}$  lines as the  $\text{SO}_3$  concentration is increased. While  $\text{SO}_3$  was hypothesized to influence the mercury capture, the results indicate that it actually does not have a significant effect on the saturated samples, and in order to understand this phenomena, the mechanism in which  $\text{SO}_3$  inhibits capture needs to be explored. The competition between  $\text{SO}_x$  and  $\text{Hg}^{2+}$  has been shown to be due to the formation of  $\text{S}^{6+}$  species on the surface of the carbon that occupy the basic binding sites to which  $\text{Hg}^{2+}$  normally binds (Li et al., 2017; Olson et al., 2005; Presto and Granite, 2007). Due to the significantly higher concentration of  $\text{SO}_x$  in flue gas than Hg (ppm vs ppb, respectively),  $\text{SO}_x$  can readily compete with Hg for adsorption sites on the carbon surface. The formation of sulfate species has been further reinforced with XPS analysis in which nearly 90% of the S found on the AC was hexavalent (Olson et al., 2005; Presto and Granite, 2007). Furthermore,  $\text{SO}_3$  has been shown to have a

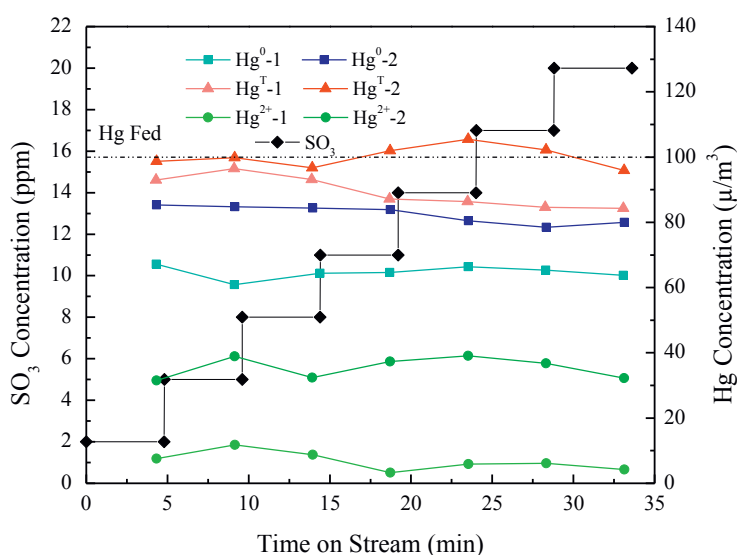


**Fig. 4 – Total ( $\text{Hg}^{\text{T}}$ ) and elemental ( $\text{Hg}^0$ ) Hg profiles for activated carbon samples exposed to Hg in simulated flue gas ( $\text{CO}_2 + \text{H}_2\text{O} + \text{N}_2 + \text{O}_2 + \text{SO}_3$ ) with the  $\text{SO}_3$  concentration increasing from 2 to 20 ppm at  $150^\circ\text{C}$  ( $\text{SO}_3$ -ramp). (This experiment was conducted upon saturating the activated carbon with Hg in simulated flue gas at  $150^\circ\text{C}$ . While the breakthrough curve is not shown here, it is similar to Fig. 3.)**

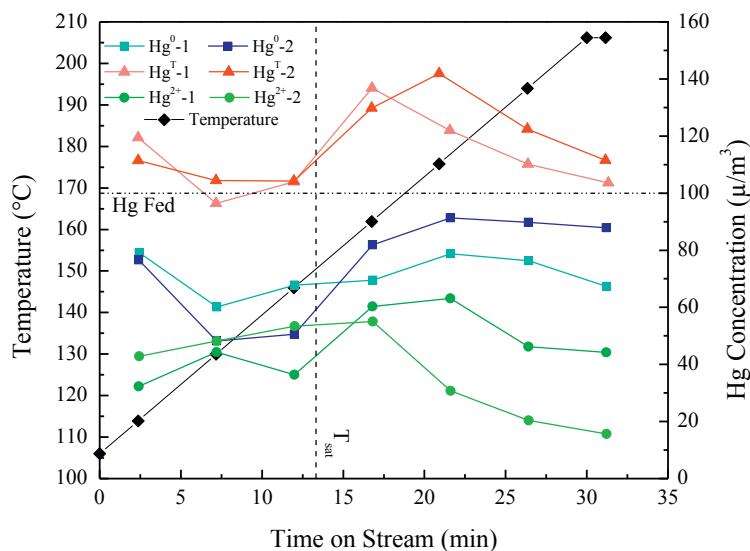


Fig. 5 – Total (Hg<sup>T</sup>) and elemental (Hg<sup>0</sup>) Hg profiles for activated carbon samples exposed to Hg in simulated flue gas (CO<sub>2</sub> + H<sub>2</sub>O + N<sub>2</sub> + O<sub>2</sub> + SO<sub>3</sub>) with 5 ppm SO<sub>3</sub> at a temperature increasing from 105°C to 205°C (T-ramp). (This experiment was conducted upon saturating the activated carbon with Hg in simulated flue gas at 150°C. While the breakthrough curve is not shown here, it is similar to Fig. 3.)

stronger effect than SO<sub>2</sub> with only 20 ppm of SO<sub>3</sub> having a much greater effect than 1000 ppm of SO<sub>2</sub> under identical exposure conditions (Presto and Granite, 2007); however, in these studies the carbon was either exposed to only SO<sub>2</sub> or only SO<sub>3</sub> or both concurrently, which is not representative of the study presented in this paper. The greater impact of SO<sub>3</sub> when compared to SO<sub>2</sub> has been explained previously by Presto and Granite (2007). First, due to the lower vapor

pressure of SO<sub>3</sub>, it is expected to more readily adsorb to the surface than SO<sub>2</sub>. Additionally, SO<sub>2</sub> can adsorb to the surface via chemisorption or physisorption while they hypothesize that SO<sub>3</sub> only chemisorbs to the surface as S<sup>6+</sup> species as SO<sub>3</sub> is already in the S<sup>6+</sup> oxidation state, essentially meaning that SO<sub>3</sub> has a higher propensity for forming S<sup>6+</sup> species that compete with Hg for Lewis base sites on the carbon (Presto and Granite, 2007). However, SO<sub>2</sub> is also able to be oxidized to

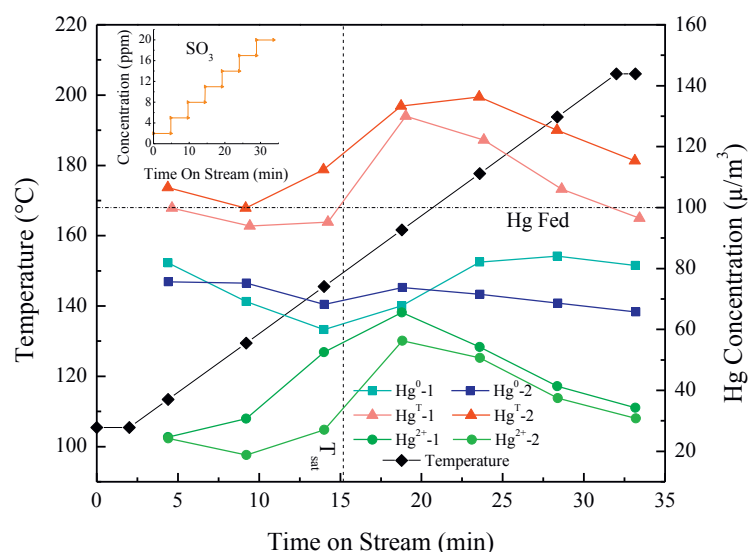


Fig. 6 – Total (Hg<sup>T</sup>) and elemental (Hg<sup>0</sup>) Hg profiles for activated carbon samples exposed to Hg in simulated flue gas (CO<sub>2</sub> + H<sub>2</sub>O + N<sub>2</sub> + O<sub>2</sub> + SO<sub>3</sub>) with the SO<sub>3</sub> concentration increasing from 2 to 20 ppm while also ramping the temperature from 105°C to 205°C (T + SO<sub>3</sub>-ramp). (This experiment was conducted upon saturating the activated carbon with Hg in simulated flue gas at 150°C. While the breakthrough curve is not shown here, it is similar to Fig. 3.)

SO<sub>3</sub> via a reaction with oxygen atoms on the surface of the carbon. This might have led to the carbon becoming saturated with S<sup>6+</sup> species during the Hg saturation experiments in presence of SO<sub>2</sub>, long before exposure to gaseous SO<sub>3</sub> for the SO<sub>3</sub>-ramp experiments, which mitigated any effects SO<sub>3</sub> would have had on the carbon.

### 2.2.2. Change in temperature (T-ramp)

The next set of experiments were conducted applying a temperature ramp from 105°C to 205°C at a rate of 3.33 °C/min while keeping the SO<sub>3</sub> concentration constant at 5 ppm and the results are presented in Fig. 5. Unlike the SO<sub>3</sub> ramp, temperature appears to have a considerable effect on Hg re-emission. The first three points of the Hg<sup>T</sup> lines show a slight decrease in the Hg concentration as the temperature is below the temperature at which saturation occurred (T<sub>Sat</sub> = 150 °C), represented by the dashed line. After ~13 min, the samples begin to re-emit some of the previously captured mercury, in conjunction with the samples' temperatures rising above T<sub>Sat</sub>. However, after experiencing peak re-emission between 160°C and 180°C, the Hg values begin to decrease to those of the Hg feed. This is intriguing as it shows that Hg is not being perpetually re-emitted as the sample is heated above the saturation temperature, but instead reaches a maximum at temperatures slightly above the saturation one. This behavior was observed in the both experiments repeated on different days.

Examining the Hg<sup>0</sup> and Hg<sup>2+</sup> profiles can reveal information regarding oxidized Hg being released from the AC. Both Hg<sup>2+</sup> and Hg<sup>0</sup> lines peak about the same temperature as the Hg<sup>T</sup> levels peak around 20 min, indicating that both Hg<sup>0</sup> and Hg<sup>2+</sup> could be re-emitting. However, at higher and higher temperatures, Hg<sup>2+</sup> decreases significantly along with Hg<sup>T</sup> while Hg<sup>0</sup> experiences minimal decrease, which could mean that the majority of the released Hg is oxidized. Previous studies have also shown that prolonged exposure to elevated temperatures results in Hg re-emission with a larger amount of Hg<sup>2+</sup> being re-emitted comparing to Hg<sup>0</sup>, which is attributed to Hg<sup>0</sup> being bonded more strongly on AC than Hg<sup>2+</sup> (Luo et al., 2006). This is consistent with the Hg<sup>2+</sup> re-emission observed in this study as a result of the temperature ramp applied to simulate the start-up conditions.

### 2.2.3. Change in temperature and SO<sub>3</sub> concentration (T + SO<sub>3</sub>-ramp)

The last condition investigated involved ramping both SO<sub>3</sub> and temperature with the results shown in Fig. 6. The inset graph in Fig. 6 shows the SO<sub>3</sub> concentration changing from 2 to 20 ppm, while the main graph shows the temperature profile from 105°C to 205°C. The first thing noticeable from the figure is its similarity to Fig. 5 (T-ramp results) with both graphs showing the same trends and features. Fig. 6 again displays how the Hg<sup>T</sup> concentration slightly decreases at low temperature and SO<sub>3</sub> values, peaks at moderate temperatures and SO<sub>3</sub> values, and finally decreases to feed levels at high temperature and SO<sub>3</sub> concentration along with a decrease in Hg<sup>2+</sup> levels while Hg<sup>0</sup> experiences minimal change. The comparison of Figs. 5 and 6 indicates that temperature is the driving factor in regard to Hg re-emission from the AC samples that are already saturated and the effect of SO<sub>3</sub>

is not considerable, similar to what was observed from the SO<sub>3</sub>-ramp experiments conducted at constant temperature.

## 3. Conclusions

Several conclusions can be drawn from the experiments conducted. The first is that SO<sub>3</sub> has minimal effect on Hg re-emission by itself. As mentioned previously, this is likely due to the fact that the samples were saturated with S<sup>6+</sup> species under a SO<sub>2</sub>-containing flue gas environment. Additionally, as observed in the preliminary Hg saturation tests, SO<sub>2</sub> greatly inhibits Hg adsorption by lowering the capture capacity of the AC.

On the other hand, temperature did play a role in the re-emission of Hg since only increased temperatures seem capable of desorbing Hg from the surface. However, this re-emission is limited with peak re-emission occurring shortly after the temperature ramp passes the saturation temperature. After passing the point of peak re-emission, the fraction of Hg<sup>2+</sup> begins decreasing with further increase in temperature that coincides with the decrease in Hg<sup>T</sup>. Since more Hg<sup>2+</sup> is released during peak re-emission, it could be concluded that Hg<sup>0</sup> is bonded to the AC surface more strongly than Hg<sup>2+</sup>. The same trends in T-ramp experiments were also observed during the T + SO<sub>3</sub>-ramp experiments.

While much work is yet to be done, the results here offer insight into the impact of the investigated parameters on Hg re-emission from AC. Future work can be performed to look into surface characterization to examine how, if at all, SO<sub>3</sub> or temperature impact surface speciation of adsorbed mercury or sulfur species, aiding in the understanding of the Hg capture/emission mechanism. Commercially available sulfur oxide tolerant carbons for mercury capture can also be investigated in future research (Granite et al., 2015).

## Acknowledgements

The authors would like to acknowledge the financial support provided by Electric Power Research Institute (EPRI), along with Ramsay Chang who provided guidance for this project. In addition, the undergraduate student who worked on this project was funded through the Research Experiences for Undergraduates (REU) Program of the National Science Foundation (award number 1358931). The authors would also like to thank ADA Carbon Solutions for providing the AC samples and Joe Wong for valuable discussions.

## REFERENCES

- Bolate, Y., 2017. Inventory of US Sources of Mercury Emissions to the Atmosphere. Columbia University.
- Carey, T.R., Jr, O.W.H., Richardson, C.F., Chang, R., Meserole, F.B., 1998. Factors affecting mercury control in utility flue gas using activated carbon. *J. Air Waste Manage. Assoc.* 48, 1166–1174.
- De, M., Azargohar, R., Dalai, A.K., Shewchuk, S.R., 2013. Mercury removal by bio-char based modified activated carbons. *Fuel* 103, 570–578.

- EIA (Energy Information Administration), 2018. Electric Power monthly. Available: <https://www.eia.gov/electricity/monthly/archive/february2018.pdf>. Accessed: August 30, 2018.
- EPRI, 2015. Utility Pulse Jet Baghouse Performance 2015 Update, 3002006153. Palo Alto, CA.
- Eswaran, S., Stenger, H.G., 2005. Understanding mercury conversion in selective catalytic reduction (SCR) catalysts. *Energy Fuel* 19, 2328–2334.
- Ghorishi, S.B., Sedman, C.B., 1998. Low concentration mercury sorption mechanisms and control by calcium-based sorbents: application in coal-fired processes. *J. Air Waste Manage. Assoc.* 48, 1191–1198.
- Granite, Evan J., Hargis, R.A., Pennline, Henry W., 1998. Sorbents for mercury removal from flue gas. Federal Energy Technology Center, Pittsburgh <https://www.osti.gov/scitech/biblio/1165/>.
- Granite, E.J., Pennline, H.W., Hargis, R.A., 2000. Novel sorbents for mercury removal from flue gas. *Ind. Eng. Chem. Res.* 39, 1020–1029.
- Granite, E.J., Freeman, M.C., Hargis, R.A., O'Dowd, W.J., Pennline, H.W., 2007. The thief process for mercury removal from flue gas. *J. Environ. Manag.* 84, 628–634.
- Granite, E.J., Pennline, H.W., Senior, C., 2015. Mercury control: For coal-derived gas streams. John Wiley & Sons.
- Ho, T.C., Yang, P., Kuo, T.H., Hopper, J.R., 1998. Characteristics of mercury desorption from sorbents at elevated temperatures. *Waste Manag.* 18, 445–452.
- Kamata, H., Ueno, S.-i., Sato, N., Naito, T., 2009. Mercury oxidation by hydrochloric acid over TiO<sub>2</sub> supported metal oxide catalysts in coal combustion flue gas. *Fuel Process. Technol.* 90, 947–951.
- Kampa, M., Castanas, E., 2008. Human health effects of air pollution. *Environ. Pollut.* 151, 362–367.
- Korpiel, J.A., Vidic, R.D., 1997. Effect of sulfur impregnation method on activated carbon uptake of gas-phase mercury. *Environ. Sci. Technol.* 31, 2319–2325.
- Li, Y., Duan, Y., Wang, H., Zhao, S., Chen, M., Liu, M., et al., 2017. Effects of acidic gases on mercury adsorption by activated carbon in simulated oxy-fuel combustion flue gas. *Energy Fuel* 31, 9745–9751.
- Luo, Z., Hu, C., Zhou, J., Cen, K., 2006. Stability of mercury on three activated carbon sorbents. *Fuel Process. Technol.* 87, 679–685.
- Miller, S.J., Dunham, G.E., Olson, E.S., Brown, T.D., 2000. Flue gas effects on a carbon-based mercury sorbent. *Fuel Process. Technol.* 65–66, 343–363.
- Min, H., Ahmad, T., Lee, S.-S., 2017. Mercury adsorption characteristics as dependent upon the physical properties of activated carbon. *Energy Fuel* 31, 724–729.
- Mullett, M., Pendleton, P., Badalyan, A., 2012. Removal of elemental mercury from Bayer stack gases using sulfur-impregnated activated carbons. *Chem. Eng. J.* 211–212, 133–142.
- Ochiai, R., Uddin, M.A., Sasaoka, E., Wu, S., 2009. Effects of HCl and SO<sub>2</sub> concentration on mercury removal by activated carbon sorbents in coal-derived flue gas. *Energy Fuel* 23, 4734–4739.
- Olson, E.S., Crocker, C.R., Benson, S.A., Pavlish, J.H., Holmes, M.J., 2005. Surface compositions of carbon sorbents exposed to simulated low-rank coal flue gases. *J. Air Waste Manage. Assoc.* 55, 747–754.
- Presto, A.A., Granite, E.J., 2007. Impact of sulfur oxides on mercury capture by activated carbon. *Environ. Sci. Technol.* 41, 6579–6584.
- Presto, A.A., Granite, E.J., 2008. Noble metal catalysts for mercury oxidation in utility flue gas. *Platin. Met. Rev.* 52, 144–154.
- Presto, A.A., Granite, E.J., Karash, A., 2007. Further investigation of the impact of sulfur oxides on mercury capture by activated carbon. *Ind. Eng. Chem. Res.* 46, 8273–8276.
- Qiao, S., Chen, J., Li, J., Qu, Z., Liu, P., Yan, N., et al., 2009. Adsorption and catalytic oxidation of gaseous elemental mercury in flue gas over MnOx/Alumina. *Ind. Eng. Chem. Res.* 48, 3317–3322.
- Ralston, N., 2008. Nanomaterials: Nano-selenium captures mercury. *Nat. Nanotech.* 3, 527.
- Rice, K.M., Walker, E.M., Wu, M., Gillette, C., Blough, E.R., 2014. Environmental mercury and its toxic effects. *J. Prev. Med. Public Health* 47, 74–83.
- Rumayor, M., Lopez-Anton, M.A., Díaz-Somoano, M., Martínez-Tarazona, M.R., 2015. A new approach to mercury speciation in solids using a thermal desorption technique. *Fuel* 160, 525–530.
- Rungnim, C., Promarak, V., Hannongbua, S., Kungwan, N., Namuangruk, S., 2016. Complete reaction mechanisms of mercury oxidation on halogenated activated carbon. *J. Hazard. Mater.* 310, 253–260.
- Rupp, E.C., Wilcox, J., 2014. Mercury chemistry of brominated activated carbons – Packed-bed breakthrough experiments. *Fuel* 117, 351–353.
- Sano, A., Takaoka, M., Shiota, K., 2017. Vapor-phase elemental mercury adsorption by activated carbon co-impregnated with sulfur and chlorine. *Chem. Eng. J.* 315, 598–607.
- Sasmaz, E., Kirchofer, A., Jew, A.D., Saha, A., Abram, D., Jaramillo, T.F., et al., 2012. Mercury chemistry on brominated activated carbon. *Fuel* 99, 188–196.
- Senior, C., Denison, M., Bockelie, M., Sarofim, A., Siperstein, J., He, Q., 2010. Modeling of thermal desorption of Hg from activated carbon. *Fuel Process. Technol.* 91, 1282–1287.
- Sjostrom, S., Dillon, M., Donnelly, B., Bustard, J., Filippelli, G., Glesmann, R., et al., 2009. Influence of SO<sub>3</sub> on mercury removal with activated carbon: Full-scale results. *Fuel Process. Technol.* 90, 1419–1423.
- Sun, P., Zhang, B., Zeng, X., Luo, G., Li, X., Yao, H., et al., 2017. Deep study on effects of activated carbon's oxygen functional groups for elemental mercury adsorption using temperature programmed desorption method. *Fuel* 200, 100–106.
- Tan, Z., Xiang, J., Su, S., Zeng, H., Zhou, C., Sun, L., et al., 2012. Enhanced capture of elemental mercury by bamboo-based sorbents. *J. Hazard. Mater.* 239–240, 160–166.
- U.S.EPA (United States Environmental Protection Agency), 2011. Mercury and Air Toxics Standards (MATS). Available: <https://www.epa.gov/mats>, Accessed date: 30 April 2018.
- Vainio, E., Fleig, D., Brink, A., Andersson, K., Johnsson, F., Hupa, M., 2013. Experimental evaluation and field application of a salt method for SO<sub>3</sub> measurement in flue gases. *Energy Fuel* 27, 2767–2775.
- Yan, R., Ng, Y.L., Liang, D.T., Lim, C.S., Tay, J.H., 2003. Bench-scale experimental study on the effect of flue gas composition on mercury removal by activated carbon adsorption. *Energy Fuel* 17, 1528–1535.
- Zhou, Q., Duan, Y., Chen, M., Liu, M., Lu, P., 2017. Studies on mercury adsorption species and equilibrium on activated carbon surface. *Energy Fuel* 31, 14211–14218.
- Zhu, C., Duan, Y., Wu, C.-Y., Zhou, Q., She, M., Yao, T., et al., 2016. Mercury removal and synergistic capture of SO<sub>2</sub>/NO by ammonium halides modified rice husk char. *Fuel* 172, 160–169.